



Cite this: *Chem. Commun.*, 2019, 55, 8072

Received 11th May 2019,  
Accepted 18th June 2019

DOI: 10.1039/c9cc03577j

rsc.li/chemcomm

# Adjustable chiral self-sorting and self-discriminating behaviour between diamond-like Tröger's base-linked cryptands†

Yuan Chen,<sup>a</sup> Cheng Qian,<sup>a</sup> Qian Zhao,<sup>a</sup> Ming Cheng,<sup>a</sup> Xinran Dong,<sup>a</sup> Yue Zhao,<sup>id</sup>\*<sup>a</sup>  
Juli Jiang<sup>id</sup>\*<sup>a</sup> and Leyong Wang<sup>id</sup>\*<sup>ab</sup>

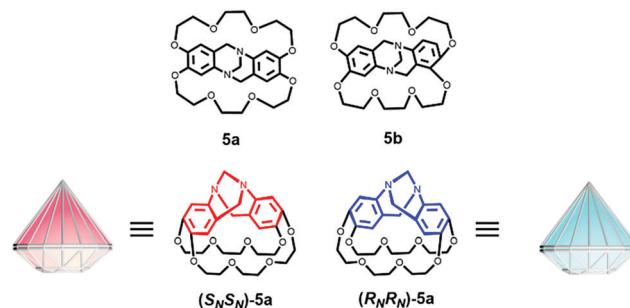
Two isomers of Tröger's base-linked cryptands **5a** and **5b** were synthesized, and both of them have two chiral N-centers, exhibiting rare diamond-like scaffolds. Particularly, when growing from the solution of *rac*-**5a**, a single enantiomer *R<sub>N</sub>R<sub>N</sub>*-**5a** was found in the crystal cell, revealing chiral self-sorting behaviour. However, when adding CF<sub>3</sub>COOH to protonate Tröger's base in the solution of *rac*-**5a**, two enantiomers were both formed in pairs in the crystal cell, exhibiting chiral self-discriminating behaviour.

Since the birth of supramolecular chemistry, a large number of macrocycles<sup>1</sup> have been constructed and used in molecular machines,<sup>2</sup> interlocked structures,<sup>3</sup> supramolecular catalysis,<sup>4</sup> metal detection,<sup>5</sup> adsorptive separation,<sup>6</sup> and smart materials widely.<sup>7</sup> Among them, chiral macrocyclic structures have attracted much attention for their wide applications in the fields of chiral recognition,<sup>8</sup> chirality inversion,<sup>9</sup> chiral induction,<sup>10</sup> and stereo-selective self-assembly.<sup>11</sup> In general, there are two common strategies to fabricate chiral macrocyclic hosts, including (i) introducing chiral auxiliaries into the macrocyclic skeletons and (ii) eliminating the symmetry plane or inversion center in order to produce inherent chirality into the cavity-shaped macrocyclic skeletons.

As a classical example of nitrogen stereogenic center,<sup>12</sup> Tröger's base (TB)<sup>13</sup> is an inherently C<sub>2</sub>-symmetric chiral compound with two N-centered chiral units. The V-shaped structure and rigid conformation made TB a useful building block to construct various functional architectures in diverse areas such as catalysis,<sup>14</sup> molecular recognition,<sup>15</sup> optical materials,<sup>16</sup> and polymer membranes.<sup>17</sup> In 2018, Stoddart and co-workers<sup>18</sup> synthesized Tröger's base-linked polymers by *in situ* intermolecular

alkylation and cyclization of either *trans*- or *cis*-di(aminobenzo)-[18]crown-6, and evaluated their proton conduction performance in humid environments. Inspired by their research, we speculated that if the length of the glycol chain was increased, it was possible that Tröger's base-linked cryptands might be formed due to the intramolecular cyclization reactions. In most cases, macrocyclic cryptands were designed by introducing functional groups into the third arm of cryptands.<sup>19</sup> To the best of our knowledge, relatively limited attention has been paid to the synthesis of cryptands by intramolecular cyclization from rigid building blocks.<sup>20</sup>

Herein, by introducing Tröger's base functional groups, two kinds of V-shaped cryptands **5a** and **5b** via the intramolecular cyclization reactions of *trans*- or *cis*-di(aminobenzo)[24]crown-8 are reported as illustrated in Scheme 1. Each of them has a TB unit, and thus, a pair of enantiomers should exist theoretically. When growing from the solution of *rac*-**5a**, a single enantiomer *R<sub>N</sub>R<sub>N</sub>*-**5a** was found in the crystal cell, exhibiting chiral self-sorting behaviour. However, when adding CF<sub>3</sub>COOH to protonate Tröger's base in the solution of *rac*-**5a**, two enantiomers were formed in pairs in the crystal cell, exhibiting chiral self-discriminating behaviour. It was a rare example that chiral self-sorting and self-discriminating behaviour could be regulated by adding external stimuli. Chirality is the omnipresent property in nature, and deeply understanding the chiral behaviour is helpful to mimic nature's designs precisely and accurately.

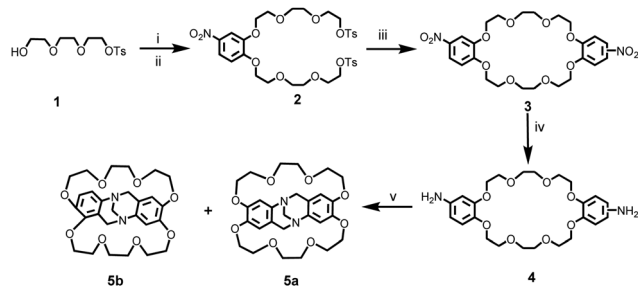


Scheme 1 Chemical structures and cartoon representations of **5a** and **5b**.

<sup>a</sup> Jiangsu Key Laboratory of Advanced Organic Materials, School of Chemistry and Chemical Engineering, Nanjing University, 163 Xianlin Avenue, Nanjing 210023, China. E-mail: zhaoyue@nju.edu.cn, jyl@nju.edu.cn

<sup>b</sup> School of Petrochemical Engineering, Changzhou University, Changzhou, 213164, China

† Electronic supplementary information (ESI) available. CCDC 1888549 and 1889896. For ESI and crystallographic data in CIF or other electronic format see DOI: 10.1039/c9cc03577j



**Scheme 2** Detailed synthetic routes for **5a** and **5b**. (i) 4-Nitrobenzene-1,2-diol,  $\text{K}_2\text{CO}_3$ ,  $\text{CH}_3\text{CN}$ , reflux; (ii)  $\text{TsCl}$ ,  $\text{Et}_3\text{N}$ ,  $\text{CH}_2\text{Cl}_2$ ,  $25^\circ\text{C}$ , total yield 73% (**2**); (iii) 4-nitrobenzene-1,2-diol,  $\text{K}_2\text{CO}_3$ ,  $\text{N}(\text{Bu})_4^+\text{I}^-$ ,  $\text{CH}_3\text{CN}$ ,  $\text{N}_2$ , reflux, 57% (**3**); (iv)  $\text{RANEY}^\text{®}\text{-Ni}$ ,  $\text{N}_2\text{H}_4\cdot\text{H}_2\text{O}$ ,  $\text{CH}_3\text{OH}$ , reflux, 82% (**4**); (v)  $\text{CF}_3\text{COOH}$ ,  $(\text{CH}_2\text{O})_n$ ,  $25^\circ\text{C}$ , 28% **5a** and 27% **5b**.

Detailed synthetic routes for cryptands **5a** and **5b** are shown in Scheme 2. By combining  $^1\text{H}$  and  $^{13}\text{C}$  nuclear magnetic resonance spectroscopy (NMR) and high-resolution mass spectrometry (HRMS), the formation of **5a** and **5b** was confirmed undoubtedly. As shown in Fig. 1, due to the  $\text{C}_2$  symmetry of **5a**, in the  $^1\text{H}$  NMR spectra of **5a** only two sets of singlets from the aromatic protons of the TB unit were found, ascribed to  $\text{H}_\text{A}$  ( $\text{H}_\text{A}'$ ) and  $\text{H}_\text{B}$  ( $\text{H}_\text{B}'$ ) at 6.78 ppm and 6.68 ppm, respectively. Compared with **5a**, in the  $^1\text{H}$  NMR spectra of **5b**, two singlets ( $\text{H}_\text{a}$  and  $\text{H}_\text{b}$ ) and two doublets ( $\text{H}_\text{c}$  and  $\text{H}_\text{d}$ ) from the aromatic protons of the TB unit were found. At the same time, the coupling constant  $J = 8.8\text{ Hz}$  was ascribed to *ortho*-coupling between protons  $\text{H}_\text{c}$  and  $\text{H}_\text{d}$ . The pair of singlets located at 6.47 ppm and 7.05 ppm belong to protons  $\text{H}_\text{a}$  and  $\text{H}_\text{b}$ , respectively. In Fig. 1(b), twelve singlets from different carbons in the aromatic area were obviously recognized in the  $^{13}\text{C}$  NMR spectra of **5b**, while six singlets from carbons in the aromatic area were recognized in the **5a** spectra. In addition, the correlations were observed in the  $^1\text{H}$ - $^{13}\text{C}$  HSQC/HMBC spectra (see the ESI,<sup>†</sup> Fig S16). Furthermore, the electrospray ionization (ESI) mass spectra provided signal peaks at  $m/z$  537.2218 and 537.2213 for  $[\text{5a} + \text{H}]^+$  and  $[\text{5b} + \text{H}]^+$ , respectively.

Both **5a** and **5b** have two chiral N-centers, and due to the bridged methylene groups of diazocine nitrogen atoms there are two enantiomers,  $(R_\text{N}R_\text{N})$ - and  $(S_\text{N}S_\text{N})$ -, which exist simultaneously in the racemate. Much effort was made to get the crystal from the solution of *rac*-**5b**, but failed. Single crystals were successfully obtained by slow diffusion of isopropyl ether into a dichloromethane solution of *rac*-**5a**, and randomly, one single crystal was selected to be analysed by X-ray. Unexpectedly, only enantiomer  $(R_\text{N}R_\text{N})$ -**5a** was found to exist in the crystal cell, and enantiomer  $(S_\text{N}S_\text{N})$ -**5a** was not found at all. Although the  $(S_\text{N}S_\text{N})$ -**5a** crystal cell was not selected by chance, it is reasonable to assume that the crystal with only the  $(S_\text{N}S_\text{N})$ -**5a** enantiomer should exist among crystals of **5a**. Due to the almost same crystalline morphologies of two **5a** enantiomers, their manual sorting was unsuccessful. Compared with the racemic mixtures of enantiomers reported during crystallization in most solutions, chiral self-sorting behaviour, or known as "conglomerate", was not so common, especially chiral self-sorting behaviour occurred between macrocycles.<sup>21–24</sup>

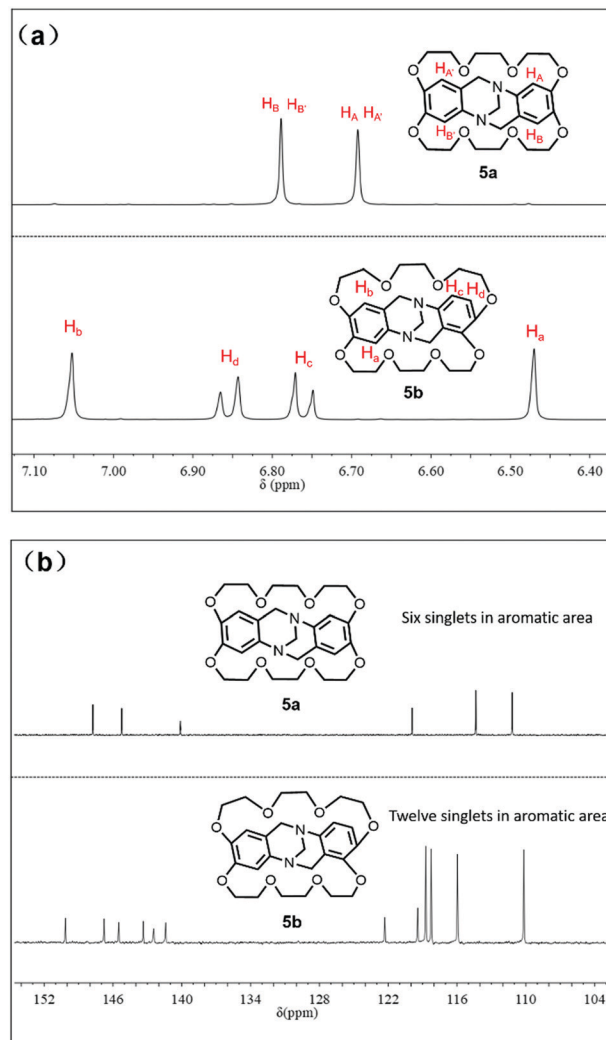


**Fig. 1** (a) Annotated  $^1\text{H}$  NMR spectrum of **5a** and **5b** (400 MHz,  $\text{CDCl}_3$ , 298 K). (b) Annotated  $^{13}\text{C}$  NMR spectrum of **5a** and **5b** (100 MHz,  $\text{CDCl}_3$ , 298 K).

As shown in Fig. 2, enantiomer  $(R_\text{N}R_\text{N})$ -**5a** crystallized in the orthorhombic unit with the  $\text{C}222_1$  space group with the  $\text{C}_2$  axis passing through the  $a$  axis, and revealed the strained rigid isosceles geometries with vertex angles of  $\sim 88^\circ$ . Defined by the base-to-apex distance, the cavity size of  $(R_\text{N}R_\text{N})$ -**5a** was 4.1 Å, and the distance of the base and hypotenuse was 6.8 Å and 6.1 Å, respectively. The favourable  $\text{C}-\text{H}\cdots\pi$  interaction ( $d_{\text{Cg}\cdots\text{C}} = 3.83\text{ Å}$  and  $\theta_{\text{C}-\text{H}\cdots\text{Cg}} = 138.8^\circ$ ) between the H atom on one of the outward glycol chains and the centroid of another phenylene ring was found as the main driving force in the stacking state of  $(R_\text{N}R_\text{N})$ -**5a**. In most cases, the crystal from the solution of the racemic compound was composed of a pair of enantiomers, and only 5 to 10 percent of racemates were crystallized in the form of condensed crystals (conglomerate crystallization).<sup>25</sup>

As the medium base, Tröger's base unit could be protonated easily.<sup>26</sup> If Tröger's base unit in *rac*-**5a** was protonated, more additional potential driving forces such as H-bonds would be involved during the crystallization, which might change the

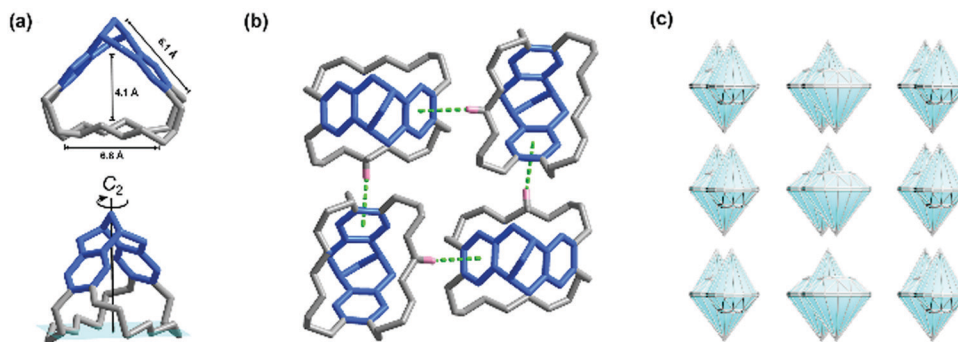


Fig. 2 (a) Front and side views of a single-crystal of  $(R_N R_N)$ -**5a**. (b) Crystal superstructures of  $(R_N R_N)$ -**5a** revealing C–H... $\pi$  interactions. (c) Cartoon representations of crystal superstructures of  $(R_N R_N)$ -**5a** (blue). Note: TB units with  $R_N R_N$  are depicted in blue, and the hydrogen is omitted for the sake of clarity.

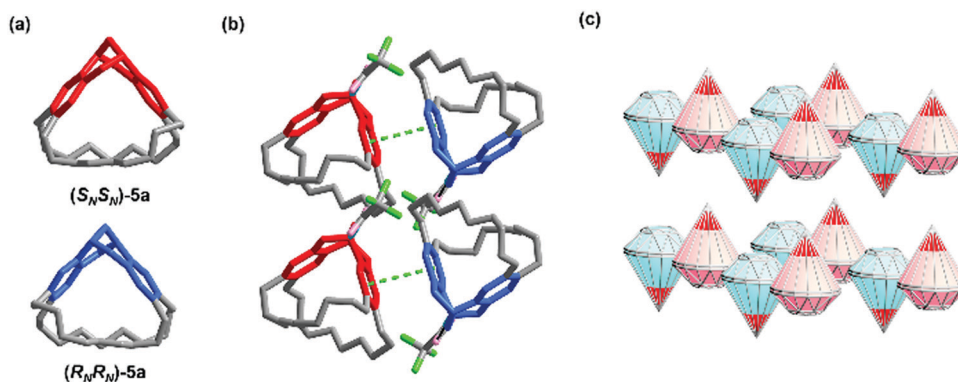


Fig. 3 (a) Crystal structures of protonated  $rac$ -[**5a-H**]. (b) Solid state superstructure of protonated  $rac$ -[**5a-H**]. (c) Cartoon representations of crystal superstructures of  $rac$ -[**5a-H**]. Note: TB units with  $S_N S_N$  are depicted in red, while TB units with  $R_N R_N$  are shown in blue, and  $CF_3COO^-$  as a counter ion is depicted in green.

chiral self-sorting behaviour in the stacking state. Along this line of consideration, 2.0 equiv. trifluoroacetic acid (TFA) was added into the solution to protonate  $rac$ -**5a**. And then, by slow diffusion of isopropyl ether into dichloromethane solution of the protonated  $rac$ -[**5a-H**], single crystals suitable for X-ray analysis were successfully obtained. Although 2.0 equiv. TFA was added into the solution to protonate  $rac$ -**5a**, only one nitrogen atom was protonated by TFA, which was consistent with the previously reported results.<sup>26</sup> Protonated  $rac$ -[**5a-H**] crystallized in the triclinic unit with the  $P\bar{1}$  space group, and the trifluoroacetate anion  $CF_3COO^-$  as a counter ion was located outside the cryptand's cavity near the tertiary ammonium N–H

group by hydrogen bonding ( $d_{N\cdots O} = 2.61 \text{ \AA}$  and  $\theta_{N-H\cdots O} = 176.5^\circ$ ). As shown in Fig. 3, [5a-H] adjusted its shape to complement adjacent quaternary ammonium centres, forming asymmetrical shape of the cavity. It was found that  $\pi$ - $\pi$  stacking existed between neighbouring enantiomers with a centroid-to-centroid distance of  $4.00 \text{ \AA}$ . Unlike spontaneous deracemization during the crystallization of  $rac$ -**5a**, a pair of enantiomers, protonated  $(R_N R_N)$ -[**5a-H**] and  $(S_N S_N)$ -[**5a-H**], were both found in the stacking state, which exhibited heterochiral self-sorting behaviour. That is to say, chiral self-sorting and self-discriminating behaviour of cryptand  $rac$ -**5a** could be regulated by adding TFA (Fig. 4).

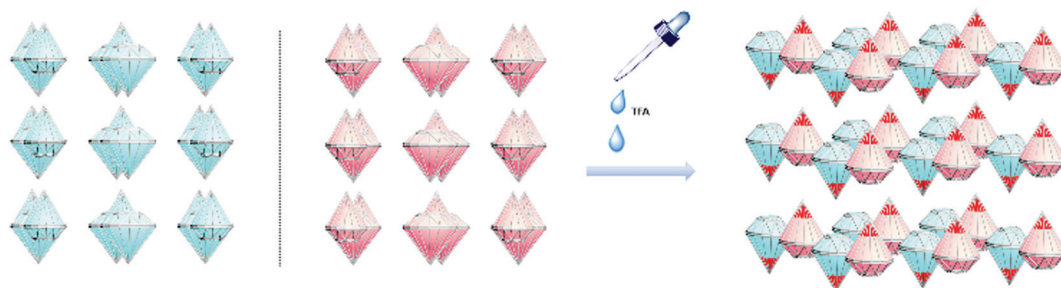


Fig. 4 Cartoon representations of chiral self-sorting and self-discriminating behaviour by adding TFA.

In summary, Tröger's base-linked cryptands **5a** and **5b**, which had unique diamond-like structures and chiral self-classification features, were synthesized using a one-step intramolecular cyclization reaction. When growing from the solution of *rac*-**5a**, a single enantiomer *R<sub>N</sub>R<sub>N</sub>*-**5a** was found in the crystal cell, exhibiting chiral self-sorting behaviour. However, when adding CF<sub>3</sub>COOH to protonate Tröger's base in the solution of *rac*-**5a**, two enantiomers were formed in pairs in the crystal cell, exhibiting chiral self-discriminating behaviour. It was not only the relative rare example that chiral self-sorting behaviour occurred between macrocycles, but also the intriguing example that chiral self-sorting and self-discriminating behaviour could be regulated by external stimuli easily.

This work was supported by the National Natural Science Foundation of China (No. 21401099, 21871135, and 21871136). We also thank Dr Srikala Pangannaya in our group for reading the manuscript.

## Conflicts of interest

There are no conflicts of interest to declare.

## Notes and references

- For examples of macrocyclic structures, see: (a) H. Yao, H. Ke, X. Zhang, S. J. Pan, M. S. Li, L. P. Yang, G. Schreckenbach and W. Jiang, *J. Am. Chem. Soc.*, 2018, **140**, 13466–13477; (b) Z. Liu, S. K. M. Nalluri and J. F. Stoddart, *Chem. Soc. Rev.*, 2017, **46**, 2459–2478; (c) T. Ogoshi, T. A. Yamagishi and Y. Nakamoto, *Chem. Rev.*, 2016, **116**, 7937–8002; (d) G. Crini, *Chem. Rev.*, 2014, **114**, 10940–10975; (e) E. J. Dale, N. A. Vermeulen, M. Juricek, J. C. Barnes, R. M. Young, M. R. Wasielewski and J. F. Stoddart, *Acc. Chem. Res.*, 2016, **49**, 262–273.
- (a) C. Cheng, P. R. McGonigal, S. T. Schneckel, H. Li, N. A. Vermeulen, C. Ke and J. F. Stoddart, *Nat. Nanotechnol.*, 2015, **10**, 547–553; (b) S. Erbas-Cakmak, D. A. Leigh, C. T. McTernan and A. L. Nussbaumer, *Chem. Rev.*, 2015, **115**, 10081–10206; (c) Y. Wang, M. Frascioni and J. F. Stoddart, *ACS Cent. Sci.*, 2017, **3**, 927–935.
- (a) Y. Akae, H. Sogawa and T. Takata, *Angew. Chem., Int. Ed.*, 2018, **57**, 14832–14836; (b) S.-H. Li, H.-Y. Zhang, X. Xu and Y. Liu, *Nat. Commun.*, 2015, **6**, 7590; (c) M. Xue, Y. Yang, X. Chi, X. Yan and F. Huang, *Chem. Rev.*, 2015, **115**, 7398–7501.
- (a) V. Blanco, D. A. Leigh and V. Marcos, *Chem. Soc. Rev.*, 2015, **44**, 5341–5370; (b) A. Palma, M. Artelsmair, G. Wu, X. Lu, S. J. Barrow, N. Uddin, E. Rosta, E. Masson and O. A. Scherman, *Angew. Chem., Int. Ed.*, 2017, **56**, 1–6.
- (a) D. Dai, Z. Li, J. Yang, C. Wang, J. R. Wu, Y. Wang, D. Zhang and Y. W. Yang, *J. Am. Chem. Soc.*, 2019, **141**, 4756–4763; (b) W. Liu, A. G. Oliver and B. D. Smith, *J. Am. Chem. Soc.*, 2018, **140**, 6810–6813.
- (a) K. Jie, Y. Zhou, E. Li and F. Huang, *Acc. Chem. Res.*, 2018, **51**, 2064–2072; (b) B. B. Ahuja and A. Vigalok, *Angew. Chem., Int. Ed.*, 2019, **58**, 2774–2778; (c) C. Li, B. Li, X. Huang, L. Dai, L. Cui, J. Li, X. Jia and B. Wang, *Angew. Chem., Int. Ed.*, 2019, **58**, 3885–3889.
- (a) D.-H. Qu, Q.-C. Wang, Q.-W. Zhang, X. Ma and H. Tian, *Chem. Rev.*, 2015, **115**, 7543–7588; (b) S. Wang, Z. Xu, T. Wang, T. Xiao, X.-Y. Hu, Y.-Z. Shen and L. Wang, *Nat. Commun.*, 2018, **9**, 1737; (c) A. Alsbaiee, B. J. Smith, L. Xiao, Y. Ling, D. E. Helbling and W. R. Dichtel, *Nature*, 2016, **529**, 190–194.
- G. W. Zhang, P. F. Li, Z. Meng, H. X. Wang, Y. Han and C. F. Chen, *Angew. Chem., Int. Ed.*, 2016, **55**, 5304–5308.
- (a) E. Lee, H. Ju, I.-H. Park, J. H. Jung, M. Ikeda, S. Kuwahara, Y. Habata and S. S. Lee, *J. Am. Chem. Soc.*, 2018, **140**, 9669–9677; (b) T. Ogoshi, T. Akutsu, D. Yamafuji, T. Aoki and T. A. Yamagishi, *Angew. Chem., Int. Ed.*, 2013, **52**, 8111–8115.
- (a) M. Inouye, K. Hayashi, Y. Yonenaga, T. Itou, K. Fujimoto, T. A. Uchida, M. Iwamura and K. Nozaki, *Angew. Chem., Int. Ed.*, 2014, **53**, 14392–14396; (b) K. Kano, H. Matsumoto, S. Hashimoto, M. Sisido and Y. Imanishi, *J. Am. Chem. Soc.*, 1985, **107**, 6117–6118.
- A. Schaly, Y. Rousselin, J.-C. Chambron, E. Aubert and E. Espinosa, *Eur. J. Inorg. Chem.*, 2016, 832–843.
- (a) T. Weilandt, U. Kiehne, G. Schnakenburg and A. Lützen, *Chem. Commun.*, 2009, 2320–2322; (b) J. Artacho, E. Ascic, T. Rantanen, C.-J. Wallentin, S. Dawaigher, K.-E. Bergquist, M. Harmata, V. Snieckus and K. Wärmark, *Org. Lett.*, 2012, **14**, 4706–4709; (c) U. Kiehne, T. Weilandt and A. Lützen, *Org. Lett.*, 2007, **9**, 1283–1286.
- (a) J. Tröger, *J. Prakt. Chem.*, 1887, **36**, 225–245; (b) M. A. Spielman, *J. Am. Chem. Soc.*, 1935, **57**, 583–585; (c) B. Dolenský, M. Havlík and V. Král, *Chem. Soc. Rev.*, 2012, **41**, 3839–3858.
- X. Du, Y. Sun, B. Tan, Q. Teng, X. Yao, C. Su and W. Wang, *Chem. Commun.*, 2010, **46**, 970–972.
- (a) L. Mosca, J. Čejka, B. Dolenský, M. Havlík, M. Jakubek, R. Kapláník, V. Král and P. A. Jr, *Chem. Commun.*, 2016, **52**, 10664–10667; (b) S. Shanmugaraju, C. Dabadie, K. Byrne, A. J. Savyasachi, D. Umadevi, W. Schmitt, J. A. Kitchen and T. Gunnlaugsson, *Chem. Sci.*, 2017, **8**, 1535–1546; (c) S. Shanmugaraju, B. la Cour Poulsen, T. Arisa, D. Umadevi, H. L. Dalton, C. S. Hawes, S. Estalayo-Adrian, A. J. Savyasachi, G. W. Watson, D. C. Williams and T. Gunnlaugsson, *Chem. Commun.*, 2018, **54**, 4120–4123.
- I. Neogi, S. Jhulki, A. Ghosh, T. J. Chow and J. N. Moorthy, *ACS Appl. Mater. Interfaces*, 2015, **7**, 3298–3305.
- (a) Y. Zhuang, J. G. Seong, Y. S. Do, W. H. Lee, M. J. Lee, Z. Cui, A. E. Lozano, M. D. Guiver and Y. M. Lee, *Chem. Commun.*, 2016, **52**, 3817–3820; (b) Z. G. Wang, X. Liu, D. Wang and J. Jin, *Polym. Chem.*, 2014, **5**, 2793–2800; (c) X. Ma, M. Abdulhamid, X. Miao and I. Pinnau, *Macromolecules*, 2017, **50**, 9569–9576.
- H. A. Patel, J. Selberg, D. Salah, H. Chen, Y. Liao, S. K. M. Nalluri, O. K. Farha, R. Q. Snurr, M. Rolandi and J. F. Stoddart, *ACS Appl. Mater. Interfaces*, 2018, **10**, 25303–25310.
- (a) Q. Wang, M. Cheng, Y. Zhao, L. Wu, J. Jiang, L. Wang and Y. Pan, *Chem. Commun.*, 2015, **51**, 3623–3626; (b) M. Cheng, C. Yao, Y. Cao, Q. Wang, Y. Pan, J. Jiang and L. Wang, *Chem. Commun.*, 2016, **52**, 8715–8718.
- P. Wei, H. Wang, K. Jie and F. Huang, *Chem. Commun.*, 2017, **53**, 1688–1691.
- (a) L. Pasteur, *Ann. Chim. Phys.*, 1848, **24**, 442–489; (b) J. E. Hein, B. H. Cao, C. Viedma, R. M. Kellogg and D. G. Blackmond, *J. Am. Chem. Soc.*, 2012, **134**, 12629–12636.
- L. Pérez-García and D. B. Amabilino, *Chem. Soc. Rev.*, 2002, **31**, 342–356.
- M. M. Safont-Sempere, G. Fernández and F. Würthner, *Chem. Rev.*, 2011, **111**, 5784–5814.
- A. Samanta, Z. Liu, S. K. Nalluri, Y. Zhang, G. C. Schatz and J. F. Stoddart, *J. Am. Chem. Soc.*, 2016, **138**, 14469–14480.
- C. P. Brock, W. B. Schweizer and J. D. Dunitz, *J. Am. Chem. Soc.*, 1991, **113**, 9811–9820.
- Z. Yang, R. Guo, R. Malpass-Evans, M. Carta, N. B. McKeown, M. D. Guiver, L. Wu and T. Xu, *Angew. Chem., Int. Ed.*, 2016, **55**, 11499–11502.